ANALYTICAL SCIENCES JUNE 2016, VOL. 32

Gold Nanoparticle Coated Silica Nanorods for Sensitive Visual Detection of microRNA on a Lateral Flow Strip Biosensor

Sunitha Takalkar,* Hui Xu,* Jiao Chen, Kwaku Baryeh,* Wanwei Qiu,*,*** Julia X. Zhao,** and Guodong Liu*,***†**

**Department of Chemistry and Biochemistry, North Dakota State University, Fargo, ND 58105, USA*
***Department of Chemistry, University of North Dakota, Grand Forks, ND 58202, USA*
****College of Food Science, Fujian Agriculture and Forestry University, Fuzhou, Fujian, 35002, P. R. China*

We present a rapid and highly sensitive approach for visual detection of microRNA (miRNA) using a gold nanoparticles coated silica nanorod label and lateral flow strip biosensor. Gold nanoparticles were decorated on the silica nanorod surface by a seeding and growth procedure. A single strand DNA probe was immobilized on the gold nanoparticles-silica nanorod surface by a self-assembling process, and the formed DNA-gold nanoparticles-silica nanorod conjugate was used to construct the lateral flow nucleic acid biosensor for detecting miRNA. The captured gold nanoparticles-silica nanorods by sandwich-type hybridization reactions (DNA-RNA-DNA) on the test zone of the lateral flow nucleic acid biosensor produced the characteristic color bands, enabling visual detection of miRNA. After systematic optimization, the new lateral flow nucleic acid biosensor was capable of detecting 10 pM of the miRNA target without instrumentation, which is six times lower than that obtained with the gold nanoparticle-based lateral flow nucleic acid biosensor. The gold nanoparticles coated silica nanorod thus provides a new and sensitive nanolabel for visual detection of biological molecules on the lateral flow biosensor.

Keywords Gold nanoparticle, silica nanorod, microRNA, lateral flow biosensor, visual detection

(Received November 10, 2015; Accepted January 26, 2016; Published June 10, 2016)

Introduction

MicroRNAs (miRNAs) play important roles in numerous developmental, metabolic, and disease processes for plants and animals.[1] By degrading miRNA transcripts or inhibiting protein translation, the gene expression is negatively regulated for a variety of fundamental biological processes, such as apoptosis, development, differentiation, and proliferation.[2] Moreover, miRNA has been regarded as a useful biomarker for cellular events or early disease diagnosis. Several biological processes, such as developmental timing, proliferation, differentiation, metabolism, cell maintenance and tissue identity, are regulated by miRNA. Animals that fail to produce certain mature miRNAs are unable to survive or reproduce.[3-7] It has been estimated that the human genome contains hundreds of miRNAs that are thought to regulate thousands of protein-coding genes and miRNAs are highly specific for gene regulation in a sequence-specific manner.[8] Thus, the altered expression patterns for these molecules indicate the dysregulation of important biological processes, which is often the cause of disease. Current methods for detecting miRNA include Northern blot analysis with radiolabeled probes; microarray-based methods; quantitative real-time polymerase-chain reaction-based approaches; *in situ* hybridization and high-throughput sequencing.[9] The disadvantages, such as utilizing harsh conditions for the sample pretreatment and having a high experimental cost, hinder the use of these methods for all practical applications.[10,11] Preferably, an ideal detection method should be able to detect the target quantitatively with high sensitivity using small amounts of starting material; the method should be specific enough for reproducible detection of the target miRNA; and importantly, the detection should be easy to perform without the need for expensive reagents or equipment. The novel miRNA detection strategies provide a powerful tool to not only depict the functions of these miRNA molecules in a variety of biological systems, but also to improve human health with early disease diagnostics.[12]

For point-of-care analysis of miRNAs, there are still great demands for innovative detection methods.[12] Lateral-flow biosensors are of considerable interest due to their wide application in the field of detections and their capability to obtain sequence-specific information in a faster, simpler and cheaper manner compared to traditional hybridization assays.[13] Recently, DNA-functionalized gold nanoparticles (GNPs) have been used to construct a lateral flow strip biosensor for visual detection of nucleic acid segments including DNA and miRNA.[14,15] However, the applications of those GNP-based lateral flow nucleic acid biosensors are limited by the low sensitivities. More recently, we reported a highly sensitive immunochromotography strip biosensor using a GNP coated silica-nanorod (SiNR) label.[16] The detection limit of the strip biosensor was 50 times lower than that of a GNP-based strip biosensor. Herein, we report a lateral flow nucleic acid biosensor based on GNP coated SiNR label for visually detecting low concentrations of miRNA. SiNR is used as a carrier to load

† To whom correspondence should be addressed.
E-mail: guodong.liu@ndsu.edu

numerous GNPs for signal amplification on the lateral flow nucleic acid biosensors. The visual detection of miRNA on the lateral flow nucleic acid biosensors is enhanced dramatically due to the increased number of GNPs per DNA-RNA hybridization event. The detection limit for the GNP-SiNR-based lateral flow nucleic acid biosensors is six times lower than that of GNP-based lateral flow nucleic acid biosensors. The promising properties of the GNP-SiNR-based lateral flow nucleic acid biosensors are reported in the following sections.

Experimental

Apparatus and reagents

The Airjet AJQ 3000 dispenser, Biojet BJQ 3000 dispenser, Clamshell Laminator, and the Guillotine cutting module CM 4000 used in this study were from Biodot Ltd. (Irvine, CA). Streptavidin, $HAuCl_4$, sucrose, Tween 20, Triton X-100, trisodium citrate, deoxyadenosine triphosphate (dATP), polyvinylpyrrolidone (PVP), hydroxylamine hydrochloride, 1-pentanol, TEOS, sodium chloride-sodium citrate (SSC) buffer 20× concentrate (pH 7.0), and PBS (pH 7.4) were purchased from Sigma-Aldrich (St. Louis, MO). All the other reagents were purchased from Sigma and used without further purification. Glass fibers (GFCP000800), cellulose fiber sample pads (CFSP001700), laminated cards (HF000MC100) and nitrocellulose membranes (HFB 18004 and HFB 24004) were purchased from Millipore (Billerica, MA). The target miRNAs and oligonucleotide probes used in this study were obtained from Integrated DNA Technologies, Inc. (Coralville, IA). The oligonucleotide sequences used for the miRNA detection were as follows:

Target miRNA-215 (*has-miR-215*): 5′-rArUrG rArCrC rUrArU rGrArA rUrUrG rArCrA rGrArC-3′[16]

Capture probe: 5′-ATA GGT CAT/3Bio/-3′

Control probe: 5′-/5Biosg/TGG ACA GAC-3′

Detection probe: 5′-/5ThioMC6-D/GTC TGT CAA-3′

All the chemicals used in this assay were of analytical reagent grade. All other solutions were prepared using ultrapure water from a Millipore Milli-Q water purification system (Billerica, MA).

Preparation of gold-nanoparticle coated silica nanorod (GNP-SiNR)

Synthesis of silica nanorod (SiNR). First, the SiO_2 core was synthesized through a reverse-emulsion method. Two grams of PVP were dissolved in 30.00 mL of pentanol in a conical flask by sonication for about 30 min. To the above mixture, 3.00 mL of 95% ethanol was added along with 840 µL of ultrapure water and 0.2 mL of 0.17 M sodium citrate. In the next step, 0.3 mL of TEOS and 0.5 mL of NH_4OH were added to stabilize the core, and the solution was left for 18 h under stirring. The surplus solution was removed by centrifuging the solution at 11000 rpm for 30 min followed by two ethanol washes. This synthesis resulted in the formation of SiNR which was finally suspended in water (10 mg mL^{-1} SiNR in water).

Preparation of gold-nanoparticle (GNP) seeds. Typically, 4.00 mL of 1% $HAuCl_4$ solution was added to 100.00 mL of H_2O in an ice bath, followed by the addition of 0.50 mL of 0.20 M K_2CO_3 to reduce Au(III) to Au(I). The solution is then stirred for 10 min until its color changes from yellow to light yellow or colorless. Then, 1.00 mL of freshly prepared $NaBH_4$ (0.50 mg/mL) was slowly added. The formation of a reddish solution indicated the successful synthesis of gold seeds.

Synthesis of GNP-SiNRs. The GNP-SiNRs were prepared according to the reported methods with slight modifications.[17,18] An aliquot with 1.00 mL of 10.00 mg/mL SiNR solution was added to a 40.00-mL gold-seed solution, and the mixture was stirred vigorously for 20 min. Surplus gold seeds were removed by centrifugation at a speed of 6500 rpm for 15 min. The obtained reddish precipitate was gold-seed-decorated SiNRs and was re-dispersed in 10.00 mL of water. In the gold-shell growth process, 4.00 mL of 1% $HAuCl_4$ solution and 0.025 g of K_2CO_3 were added to 90.00 mL of water. The mixture was stirred until it turned to light yellow or colorless. Then, 10.00 mL of a gold-seed-decorated SiNR solution, 1.00 mL of 0.5 M hydroxylamine hydrochloride, and 1.00 g of PVP were sequentially added to the growth solution. After overnight reaction, the solution was centrifuged at a speed of 6500 rpm for 15 min and was washed three times with water.

Preparation of DNA-GNP-SiNR conjugate. First, 10 µL of dATP was added to 1 mL of three-fold concentrated GNP-SiNR solution (the final concentration of dATP was 7.05 µM), and the mixture was incubated at room temperature for 20 min. Then, 15 µL of 1% SDS was slowly added to the mixture, and it was incubated on a shaker for another 10 min. Next, 50 µL of 2.0 M NaCl was added at a rate of 2.0 µL every 2 – 3 min. Then, one OD thiolated DNA (detection probe) was added and incubated for 3 h in a water bath at 60°C. After the incubation, the mixture was centrifuged at 8000 rpm for 5 min, and the supernatant was discarded. Then, the DNA-GNP-SiNR conjugates were washed with 1 mL of PBS three times; the resulting pellet was re-suspended in 1 mL eluent buffer (20 nM $Na_3PO_4{\cdot}12H_2O$, 5% BSA, 0.25% Tween 20 and 10% sucrose).

Preparation of streptavidin-biotinylated DNA probe conjugate. Two hundred microliters of 2.5 mg mL^{-1} streptavidin were mixed with 50 nmol biotinylated DNA probe (capture probe or control DNA probe). The mixture was incubated at room temperature for 1 h. After adding 500 µL PBS to the mixture, the solution was centrifuged for 20 min at 6000 rpm at 4°C. This step was repeated three times. The remaining solution, in a filter, was diluted to 600 µL with PBS.

Preparation of lateral-flow strip biosensor. The lateral flow strip biosensor consisted of four components: sample application pad, conjugate pad, nitrocellulose membrane, and absorbent pad.[19] All components were mounted on a common backing layer (typically an inert plastic, *e.g.*, polyester) using the Clamshell Laminator (Biodot; Irvin, CA). The sample application pad (17 mm × 30 cm) was made from glass fiber (CFSP001700, Millipore) and treated with a Tris–HCl solution (pH 8.0) containing 0.23% Triton X-100, 0.05 M Tris–HCl, and 0.15 M NaCl. After drying the pad at 37°C for 2 h, they were stored in desiccators at room temperature (RT). The streptavidin-biotinylated DNA probes were used to prepare the test zone and the control zone on the nitrocellulose membrane, and the DNA-GNP-SiNR conjugates were dispensed on the conjugate pad. The distance between the test and control zones was 3 mm. The membrane was then dried at 37°C for 1 h and stored at 4°C in a dry state. A clamshell laminator was used to assemble all the components (the sample pad, conjugate pad, nitrocellulose membrane, and absorption pad) on a plastic adhesive backing (60 mm × 30 cm) which is the final step in the preparation of the lateral flow strip biosensor. Each part overlapped 2 mm to ensure that the solution could migrate through the strip during the assay. Strips with a 3-mm width were cut using the Guillotin CM 4000 cutting module.

Analytical procedure

Sample solutions containing various concentrations of target miRNA were prepared in an eightfold, diluted SSC buffer

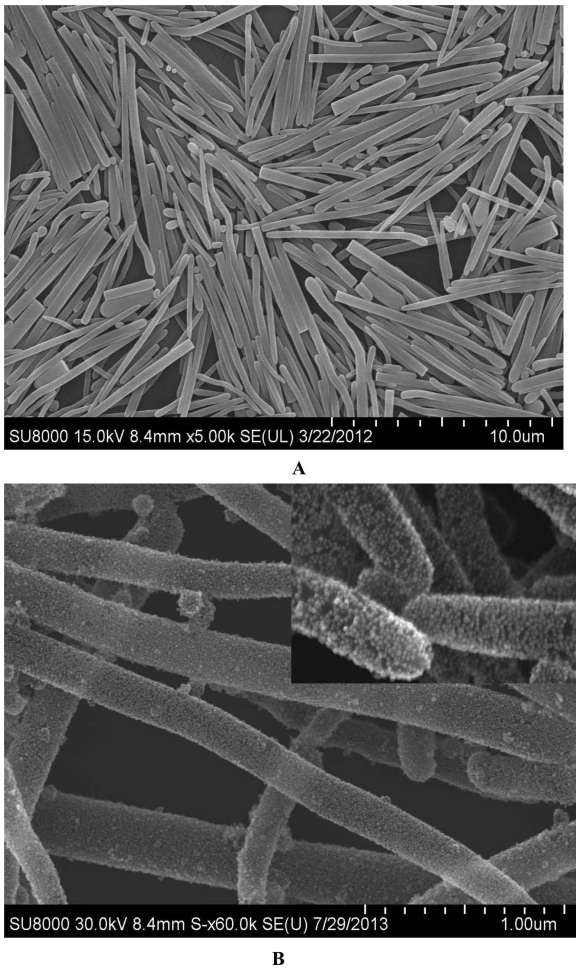

Fig. 1 SEM images of silica nanorods (A) and gold-nanoparticle-coated silica nanorods (B).

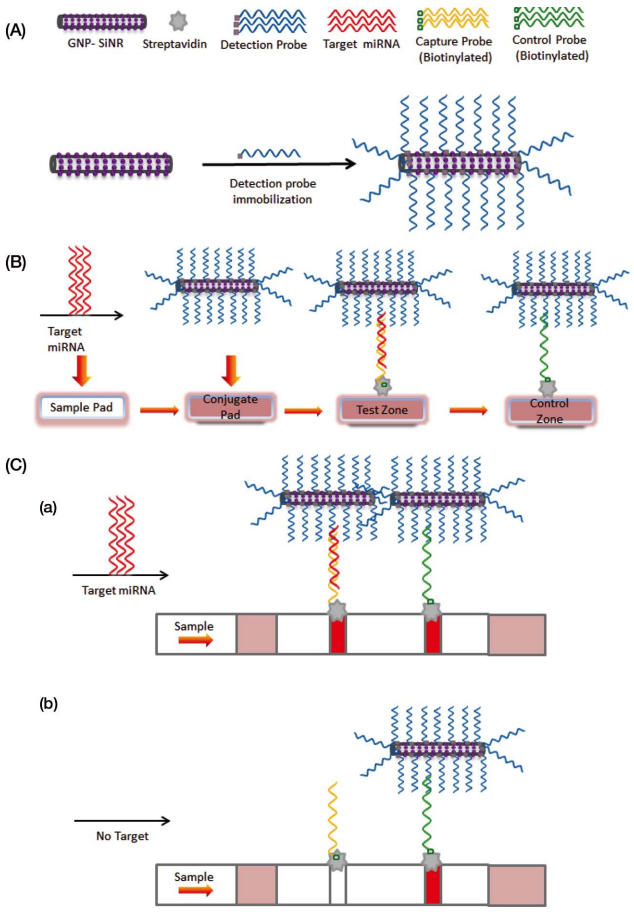

Fig. 2 (A) Schematic illustration of the preparation of GNP-SiNR DNA conjugates. (B) Schematic illustration of capturing GNP-SiNR-DNA conjugates on the test and control zones of a lateral-flow nucleic acid biosensor; GNP-SiNR-DNA conjugate is pre-dispensed on the conjugate pad, streptavidin-biotin-capture DNA and streptavidin-biotin-control DNA are pre-dispensed on the test zone and control zone of nitrocellous membrane. (C) Visualization of the signal in the presence (a) or absence (b) of target miRNA.

containing 4% BSA. In a typical test, 100 µL of the sample solution was added to the sample pad region of the lateral flow strip biosensor. The solution migrated toward the absorption pad to hydrolyze DNA-GNP-SiNR and formed miRNA-DNA-GNP-SiNR complexes. The complexes moved along the strip toward the test zone and were captured by the capture DNA probe on the test zone. The accumulation of GNP-SiNRs resulted in the color change (to purple) at the test zone. After waiting for 10 min, 30 µL running buffer (1/8 SSC + 4% BSA) was added to the sample pad to wash the lateral flow strip biosensor. For quantitative measurements, a digital camera was used to take the photo images of the lateral flow strip biosensor, and the optical intensity of the test bands was read using the Image J Viewer software.

Results and Discussion

Principle of miRNA detection using the GNP-SiNR-based lateral-flow strip biosensor

In this study, gold-nanoparticles coated silica nanorod (GNP-SiNR) was used as a new nanolabel for sensitive visual detection of miRNA on the lateral-flow strip biosensor. SiNRs with a length of 3.4 to 7.0 µm were prepared with a typical reverse-emulsion method (Fig. 1A). A two-step procedure, with GNP seeding and growth, was employed to load the GNP layer on the SiNR surface. The GNPs with a diameter of 9.7 ± 1.6 nm were first adsorbed by the PVP polymer on the SiNR surface (GNP seeding); the growth of GNPs was performed in a growth solution containing $HAuCl_4$ and hydroxylamine hydrochloride. Figure 1B presents the typical SEM images of GNP-SiNRs. One can see a layer of GNPs with a diameter of 16.7 ± 2.4 nm (see insert of Fig. 1B) covered on the SiNR surface. It was found that the GNP-SiNRs would be well-dispersed in the PBS buffer.

The principle of miRNA detection using the GNP-SiNR nanolabels is based on on-strip DNA-RNA hybridization reactions to form sandwich-type DNA-miRNA-DNA-GNP-SiNR complexes, which are captured on the test zone of the lateral flow strip biosensor; the change in the color on the test zone due to the accumulation of GNPs enables the visual detection of miRNA (Fig. 2). One can expect that the use of GNP-SiNR nanolabels would increase the number of the captured GNPs per DNA-RNA hybridization event, thus an enhanced visual effect. The self-assembly reaction *via* the Au-S bond results in the immobilization of the thiolated detection DNA probe on the GNP surface of the GNP-SiNR (Fig. 2A). The DNA-GNP-SiNR conjugates were dispensed on the conjugate pad of the lateral flow strip biosensor. Streptavidin-

biotinylated capture DNA probe (complementary with a part of miRNA target) and control DNA probe (complementary with detection DNA probe on the GNP surface) were pre-dispensed on the nitrocellulose membrane to form test zone and control zone, respectively (Fig. 2B). The sample solution containing the target miRNA was applied on the sample pad (Fig. 2C(a)). The sample solution migrates by capillary action and comes in contact with the DNA-GNP-SiNR conjugates on the conjugate pad. The miRNA binds with the detection DNA probe on the GNP surface to form the miRNA-DNA-GNP-SiNR complex through a RNA-DNA hybridization reaction (Fig. 2C(b)). As the formed complexes continue to move along the strip by capillary action, they are captured by the capture DNA probes on the test zone. Thus without any instrumentation, the accumulation of GNP-SiNRs leads to the color change of the test zone, enabling visual detection of miRNA. The excess of DNA-GNP-SiNR conjugates continue to migrate and pass the control zone, where the control DNA probe (complementary with the detection DNA probe) was immobilized. Then, a second colored band forms as the excess DNA-GNP-SiNR conjugates are captured by the hybridization events between the detection DNA probe and the control DNA probe (Fig. 2C(a)). No band was observed on the test zone indicating the absence of miRNA. A band observed on the control zone is an indication that the lateral flow strip biosensor is working properly (Fig. 2C(b)).

As a proof of concept experiment, we tested the responses of 0-nM miRNA (control), 5-nM miRNA, 50-nM non-complementary miRNA and the mixture of 5-nM miRNA and 50-nM non-complementary miRNA on the GNP-SiNR-based lateral flow strip biosensors. Figure 3A presents the photo images of the lateral flow strip biosensors after the completed assays. There was no test band observed with the 0-nM miRNA and the 50-nM non-complementary miRNA while a distinct, purple band appeared in the presence of 5.0-nM miRNA. The results indicated that the proposed GNP-SiNR-based lateral flow strip biosensor would detect miRNA selectively. The selectivity was further demonstrated by detecting the response of 5-nM miRNA in the presence of 50-nM noncomplementary miRNA. It was found that the presence of excess noncomplementary miRNA does not affect the signal of target miRNA.

To demonstrate the signal amplification of GNP-SiNR nanolabels, we compared the optical responses of 0.1-nM miRNA on the GNP and GNP-SiNR-based lateral flow strip biosensors (Fig. 3B). The signal-to-noise (*S*/*N*) ratio of the GNP-SiNR-based lateral flow strip biosensor was almost six times higher than that of the GNP-based lateral flow strip biosensor. Such a significant enhancement in *S*/*N* ratio was ascribed to the higher number of captured GNPs per hybridization event on the lateral flow strip biosensor test zone. The inset of Fig. 3B presents the typical images of GNP- and GNPs-SiNR-based lateral flow strip biosensors in the presence of 0.1-nM miRNA. A distinct, purple band was seen on the test zone of the GNP-SiNR-based lateral flow strip biosensor while a weak, red band was observed on the test zone of the GNP-based lateral flow strip biosensor. The purple color was ascribed to the large size of the GNPs on the GNP-SiNR conjugates.

Optimization of assay parameters

Analytical parameters, including the volume of the DNA-GNP-SiNR on the conjugate pad, the quantities of capture DNA probes on the test zone and the components of the running buffers, would affect the lateral flow strip biosensor's response. First, we studied the effect of the DNA-GNP-SiNR conjugate

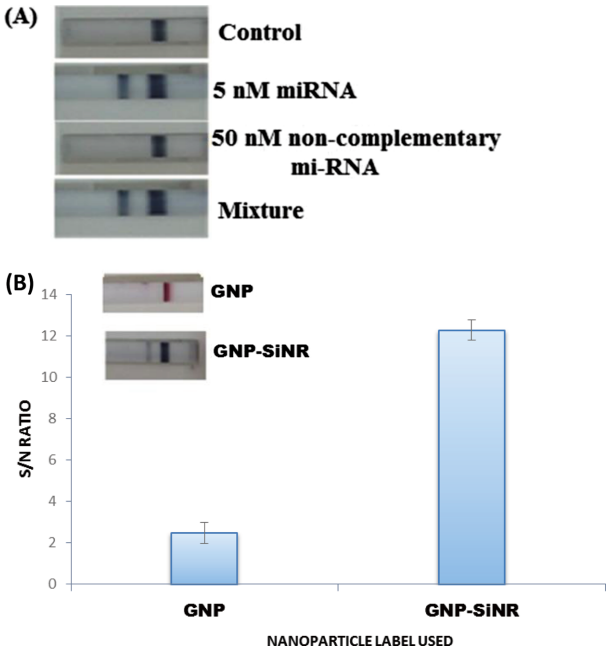

Fig. 3 (A) Typical photo images of lateral flow nucleic acid biosensors in the presence of 0-nM miRNA (control), 5.0-nM miRNA, 50-nM non-complementary miRNA and the mixture of 5.0-nM miRNA + 50-nM noncomplementary miRNA. Assay time: 30 min. (B) Histogram for the response of 0.1-nM miRNA using GNP and GNP-SiNR nanolabels. Inset: Corresponding photo images of the GNP-based (above) and GNP-SiNR-based lateral flow nucleic acid biosensors (below).

volume on the *S*/*N* ratio of the lateral flow strip biosensor, which was the ratio of the test-line intensities in the presence of a particular concentration of miRNA *versus* the absence of miRNA. To obtain the best *S*/*N* ratio, the DNA-GNP-SiNR on the conjugate pad was optimized by loading different volumes of DNA-GNP-SiNR on the conjugate pad. Figure 4A presents the effect of conjugate volume on the *S*/*N* ratio of the lateral flow strip biosensor. It can be seen that the *S*/*N* ratio increased with the increase of conjugate volume up to 5.0 μL; a further increase resulted in a decrease of the *S*/*N* ratio. The decrease of *S*/*N* ratio at a larger conjugate volume may be attributed to a saturation of signal intensity and increased nonspecific adsorption due to the presence of excess conjugates. Therefore, 5.0 μL of DNA-GNP-SiNR conjugate was used as the optimal conjugate volume throughout the entire study.

The amount of capture DNA probes at the test zone of the lateral flow strip biosensor also affects the response of miRNA. In the current study, the quantities of capture DNA were optimized by dispensing different amounts of streptavidin-biotinylated DNA complexes. The effect of the capture DNA amount (dispensing cycles) on the lateral flow strip biosensor's *S*/*N* ratio is shown in Fig. 4B. The highest *S*/*N* ratio was obtained with four dispensing cycles, which was then used in the following assays. The decreased *S*/*N* with more dispensing cycles may be caused by the increased background signal.

The nitrocellulose membrane is one of the most important materials for preparing the lateral flow strip biosensor. There are two types of nitrocellulose membranes: 3- and 4-min membranes. The time indicates the movement time of the sample solution from the sample pad to the absorption pad. We compared the *S*/*N* ratios of the lateral flow strip biosensors (Fig. 4C) and found that the 3-min membrane showed a higher

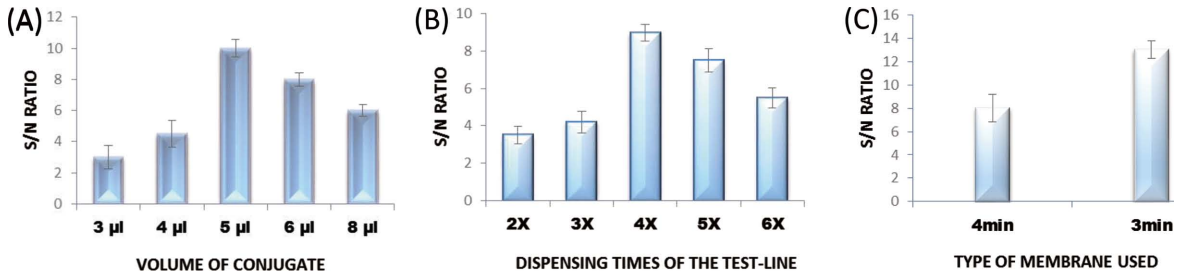

Fig. 4 (A) The effect of conjugate volume on the response of lateral flow nucleic acid biosensors. (B) Effect of dispensing times on the response of lateral flow nucleic acid biosensors. (C) Optimization for the type of nitrocellulose membrane used. miRNA-215 concentration: 0.1 nM.

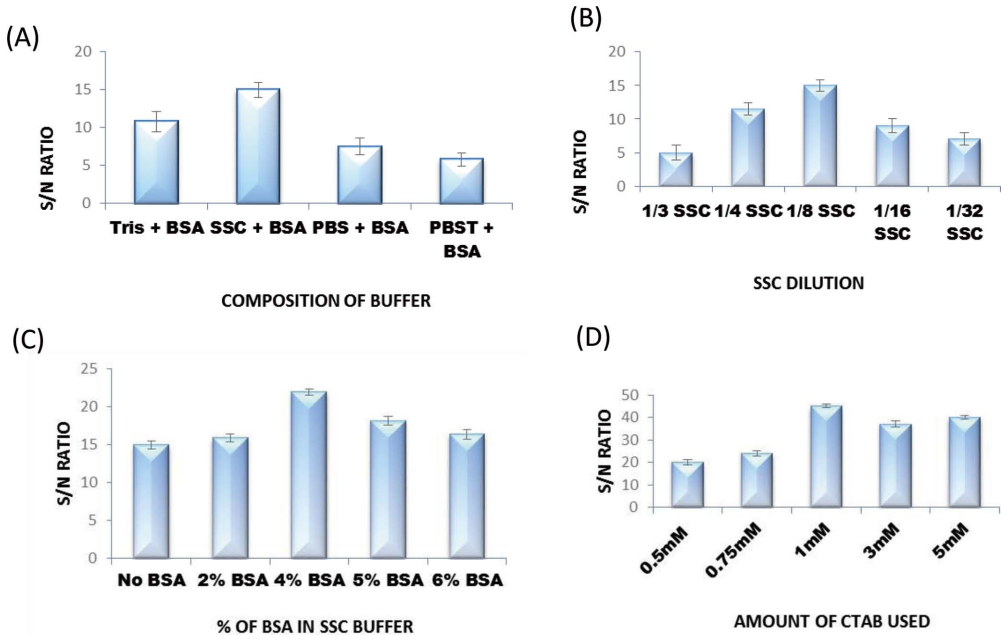

Fig. 5 Effect of buffer on the performance of lateral flow nucleic acid biosensors: (A) different buffers used; (B) SSC concentrations in the buffer (C); BSA concentrations in the buffer; (D) CTAB concentrations in the buffer. miRNA-215 concentration: 0.1 nM

S/N ratio. This might be due to the difference in the pore size of the membranes, which would affect the movement of GNP-SiNR-DNA conjugates. The pore size of 3-min membrane is larger than that of 4-min membrane. Larger pore size of the membrane would facilitate the movement of silica nanrods on the membrane and reduce the nonspecific adsorption, thus resulting in a higher *S/N* ratio.

The composition of the running buffer plays a very important role to minimize the nonspecific adsorption of nanolabels and increases the hybridization efficiency. PBS (1% BSA), PBST (1% BSA), Tris-HCl (1% BSA) and SSC (1% BSA) were used as running buffer and the *S/N* ratios were compared (Fig. 5A). It was found that the highest *S/N* ratio was obtained with SSC+1% BSA buffer. We also optimized the concentrations of SSC and BSA to further improve the *S/N* ratio of the lateral flow strip biosensor (Figs. 5B and 5C). The SSC buffers were prepared by diluting the stock SSC buffer solution (3 M, Sigma-Aldrich) with different dilution times that ranged from 4 to 32 times. BSA concentrations in the running buffer varied from 1 to 4%. One can see the *S/N* ratio of the lateral flow strip biosensor increased with the increase of BSA concentration. The highest *S/N* ratio was obtained with the 1/8 SSC buffer containing 4% BSA. The decreased *S/N* with higher BSA concentration may be caused by the increased nonspecific adsorption of GNP-SiNR-DNA on the test zone, thus the increased background signal.

During the optimization, we noticed that some conjugates remained on the conjugate pad and that the assay time was longer than for the GNP-based lateral flow strip biosensor. It might be caused by the large size of the SiNRs. To facilitate better movement of the DNA-GNP-SiNR conjugates across the lateral flow strip biosensor, CTAB (a surfactant) was added to the running buffer. It was found that the GNP-SiNR-DNA conjugate was stable in the presence of CTAB surfactants. Removal of CTAB results in the aggregation of conjugates making it difficult to move. The CTAB concentration in the running buffer was thus optimized (Fig. 5D). The highest *S/N* ratio for the lateral flow strip biosensor was obtained with 1-mM CTAB. Higher concentrations of CTAB would increase the viscosity of the running buffer and the nonspecific adsorption of GNP-SiNR-DNA on the test zone, and thus result in a decreased *S/N* ratio.

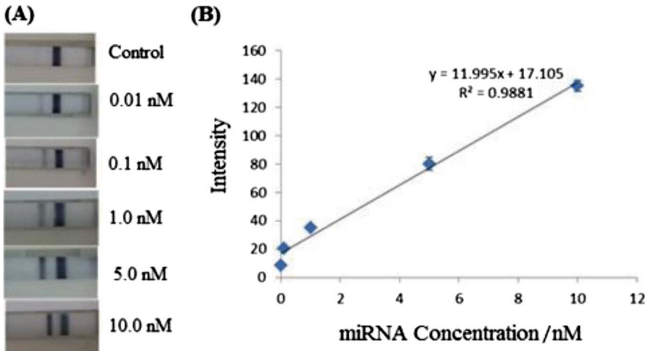

Fig. 6 Photo images: (A) the lateral flow nucleic acid biosensors with different concentrations of the target under optimal experimental conditions and (B) optical responses of the test bands on the lateral flow nucleic acid biosensors's test zones.

Analytical performance

After the optimizations of the DNA-GNP-SiNR conjugate amount (5 μL), the amount of capture probe (four dispensing cycles) and the components of running buffer (1/8 SSC + 4% BSA + 1 mM CTAB), the GNP-SiNR-based lateral flow strip biosensor was assessed by detecting different concentrations of target miRNA-215, ranging from 0 to 100 nM. The photo images of the lateral flow strip biosensors were taken by a digital camera and the intensities of the bands were obtained by using the Image J viewer software. Figure 6A shows the typical photo images of lateral flow strip biosensors after applying the sample solutions containing miRNA concentrations. No test band was observed in the control test (0 nM miRNA), indicating the nonspecific adsorption was negligible under the optimized experimental conditions. The intensities of the test bands increased with the increase of miRNA-215 and the threshold of visual detection was 0.01-nM (10 pM). The calibration curve was plotted using the peak areas *versus* the microRNA-215 concentration (Fig. 6B). A good linearity relationship was obtained over the 0.01 to 10 nM range, and the detection limit was estimated to be 0.01 nM ($S/N = 3$). This detection limit is a six-fold improvement compared to the GNP-based lateral flow strip biosensor.[14] In addition to high sensitivity, the GNP-SiNR-based lateral flow strip biosensor also exhibited high reproducibility. The reproducibility of the lateral flow strip biosensor was studied by testing the lateral flow strip biosensors in the absence and presence of 5.0-nM target miRNA-215. Each sample was tested six times with six different lateral flow strip biosensors, and one could see that similar responses were obtained at the same concentration level. The relative standard deviations (RSD) of the signal for control and 5-nM were 2.8 and 3.0%, respectively, which indicates a good reproducibility of the measurements.

Conclusion

The present study reported a new nanolabel, gold-nanoparticle-coated silica nanorod (GNP-SiNR), for visually detecting miRNA on a lateral-flow strip biosensor with high specificity and sensitivity. The sensitivity of the GNP-SiNR-based lateral flow strip biosensor was enhanced six times compared to the previous GNP-based lateral flow strip biosensor. After systematic optimization, the GNP-SiNR was capable of detecting 10 pM miRNA without instrumentation. The concept should be extended to visually detect protein biomarkers using the GNP-SiNR nanolabels. Further work will aim to detect miRNA in cell-lysate and biological fluids. The GNP-SiNR-based lateral flow strip biosensor, thus, provides a rapid and low-cost platform for sensitive detection of biological molecules, and shows great promise for point-of-care diagnosis of genetic and infectious diseases.

Acknowledgements

This research was supported by the National Cancer Institute (Grant No. R21CA137703) and the National Institute of General Medicine (NIGMS; 5P30 GM103332). Its contents are solely the responsibility of the authors and do not necessarily represent the official views of the NIH. J. X. Z. acknowledges financial support from the National Science Foundation (Grant Nos. CHE 0911472 and CHE 0947043).

References

1. C. M. Croce, *Nat. Rev. Genetics.*, **2009**, *10*, 704.
2. D. P. Bartel, *Cell*, **2004**, *116*, 281.
3. E. Bernstein, S. Y. Kim, M. A. Carmell, E. P. Murchison, H. Alcorn, M. Z. Li, A. A. Mills, S. J. Elledge, K. V. Anderson, and G. J. Hannon, *Nat. Genet.*, **2003**, *35*, 215.
4. R. F. Ketting, S. E. Fischer, E. Bernstein, T. Sijen, G. J. Hannon, and R. H. Plasterk, *Genes Dev.*, **2001**, *15*, 2654.
5. F. Pichiorri, S. S. Suh, A. Rocci, L. De Luca, C. Taccioli, R. Santhanam, W. Zhou, D. M. Benson, and R. H. Plasterk, *Cell*, **2006**, *124*, 877.
6. R. Shivdasani, *Blood*, **2006**, *108*, 3646.
7. E. Wienholds, M. J. Koudijs, F. J. Van Eeden, E. Cuppen, and R. H. Plasterk, *Nat. Genet.*, **2003**, *35*, 217.
8. H. Lin and H. J. Gregory, *Nat. Rev. Genetics*, **2004**, *5*, 522.
9. P. D. Mariangels and C. R. Maria, *Anal. Chim. Acta*, **2011**, *699*, 134.
10. H. Jia, Z. Li, C. Liu, and Y. Cheng, *Angew. Chem. Int. Ed.*, **2010**, *49*, 5498.
11. C. Li, Z. Li, H. Jia, and J. Yan, *Chem. Commun.*, **2011**, *47*, 2595.
12. H. Dong, J. Lei, L. Ding, Y. Wen, H. Ju, and X. Zhang, *Chem. Rev.*, **2013**, *113*, 6207.
13. J. Wang, *Biosens. Bioelectron.*, **2006**, *21*, 1887.
14. X. Gao, H. Xu, M. Baloda, A. S. Gurung, L. Xu, T. Wang, X. Zhang, and G. Liu, *Biosens. Bioelectron.*, **2014**, *54*, 578.
15. X. Mao, Y. Ma, A. Zhang, L. Zhang, L. Zeng, and G. Liu, *Anal. Chem.*, **2009**, *81*, 1660.
16. H. Xu, J. Chen, J. Birrenkott, J. X. J. Zhao, S. Takalkar, K. Baryeh, and G. Liu, *Anal. Chem.*, **2014**, *86(15)*, 7351.
17. F. Pichiorri, S. S. Suh, A. Rocci, L. De Luca, C. Taccioli, R. Santhanam, W. Zhou, D. M. Benson Jr, C. Hofmainster, and H. Alder, *Cancer Cell*, **2010**, *18*, 367.
18. S. Xu, S. Hartvickson, and J. X. Zhao, *Langmuir*, **2008**, *24*, 7492.
19. Y. He, S. Zhang, X. Zhang, M. Baloda, A. S. Gurung, H. Xu, and G. Liu, *Biosens. Bioelectron.*, **2011**, *26*, 2018.